PHILOSOPHICAL TRANSACTIONS OF THE ROYAL SOCIETY A
MATHEMATICAL, PHYSICAL & ENGINEERING SCIENCES

Transition delay using control theory

S. Bagheri and D. S. Henningson

Phil. Trans. R. Soc. A 2011 **369**, 1365-1381
doi: 10.1098/rsta.2010.0358

PHILOSOPHICAL TRANSACTIONS OF THE ROYAL SOCIETY A

Phil. Trans. R. Soc. A (2011) **369**, 1365–1381
doi:10.1098/rsta.2010.0358

Transition delay using control theory

BY S. BAGHERI AND D. S. HENNINGSON*

Linné Flow Centre, Department of Mechanics, KTH, 100 44, Stockholm, Sweden

This review gives an account of recent research efforts to use feedback control for the delay of laminar–turbulent transition in wall-bounded shear flows. The emphasis is on reducing the growth of small-amplitude disturbances in the boundary layer using numerical simulations and a linear control approach. Starting with the application of classical control theory to two-dimensional perturbations developing in spatially invariant flows, flow control based on control theory has progressed towards more realistic three-dimensional, spatially inhomogeneous flow configurations with localized sensing/actuation. The development of low-dimensional models of the Navier–Stokes equations has played a key role in this progress. Moreover, shortcomings and future challenges, as well as recent experimental advances in this multi-disciplinary field, are discussed.

Keywords: transition delay; feedback control; flat-plate boundary layer

1. Introduction

In this review, we are concerned with the control of laminar–turbulent transition using numerical simulations. The focus is mainly on the flow along a flat plate, as it is the archetype of boundary-layer flows, contains the fundamental transition physics and pertains to countless examples in both nature and industry. The key assumption underlying the investigations is that a linear model can describe the initial phase of the laminar–turbulent transition. This assumption is based on the idea that, by suppressing the growth of small-amplitude disturbances as early as possible, it may be possible to delay the entire process of transition to turbulence. Secondly, the review focuses strictly on investigations where linear control theory has been employed, and in particular optimal and robust feedback-control methods. This paper complements other reviews in the field [1–3], by keeping the presentation of algorithms and methods from control theory to a minimum. We will instead emphasize on how computationally tractable linear models of a fluid flow are devised and which fluid mechanical properties the subsequent control can achieve.

*Author for correspondence (henning@mech.kth.se).

One contribution of 15 to a Theme Issue 'Flow-control approaches to drag reduction in aerodynamics: progress and prospects'.

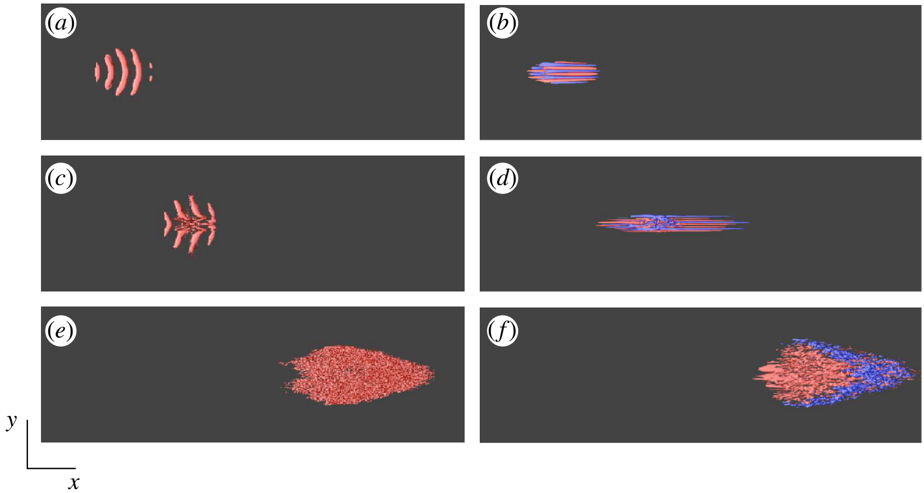

Figure 1. Snapshots of the nonlinear response (a,c,e) to a Tollmien–Schlichting (TS) disturbance and (b,d,f) to streamwise vortices at transitional Reynolds numbers ($Re_x \approx 10^5$–10^6). The flat plate is shown in black and viewed from the top. (a,c,e) Grey (red online) iso-contour levels depict the λ_2-criterion of the TS wavepacket at (a) $t = 0$, (c) $t = 300$ and (e) $t = 1000$. (b,d,f) Dark/light grey (red/blue online) iso-contour levels correspond to the positive/negative streamwise velocity component of the streak at (b) $t = 200$, (d) $t = 500$ and (f) $t = 1000$. The turbulent spots eventually leave the computational domain and the flow returns to the steady boundary layer. (Online version in colour.)

(a) *Disturbance behaviour in wall-bounded flows*

Consider a steady uniform viscous stream of flow with speed U that encounters a flat plate of length L. It is appropriate to define the Reynolds number as $Re_x = Ux/\nu$, where $0 \leq x \leq L$ is the distance on the plate from the leading edge and ν is the kinematic viscosity. The critical Reynolds number, Re_x, for the laminar–turbulent transition is notoriously difficult to determine. Transition can occur abruptly, gradually and at completely different locations on the plate, depending on the size, spatial structure and temporal behaviour of the disturbances that may be found in the laboratory or numerical experiments. For example, the presence (or combination) of acoustic waves, roughness on the plate and vortical structures in the free stream critically affects the transition process. To elucidate this sensitivity and to highlight the essential physics, we perform two numerical experiments of localized disturbances.

The first disturbance is a packet of travelling waves composed of a range of small wavelengths in the streamwise direction and a rather large wavelength in the spanwise direction (figure 1a). These nearly two-dimensional Tollmien–Schlichting (TS) wavepackets are present when the background turbulence level is extremely low (of the order of 0.05%). For sufficiently high Reynolds numbers (above 10^6), they experience a rapid breakdown, characterized by the appearance of significantly smaller spanwise wavelengths, high local shear layers and inflection points in instantaneous wall-normal velocity profiles. Figure 1a,c,e shows snapshots of the disturbance (top view of the plate) at three different

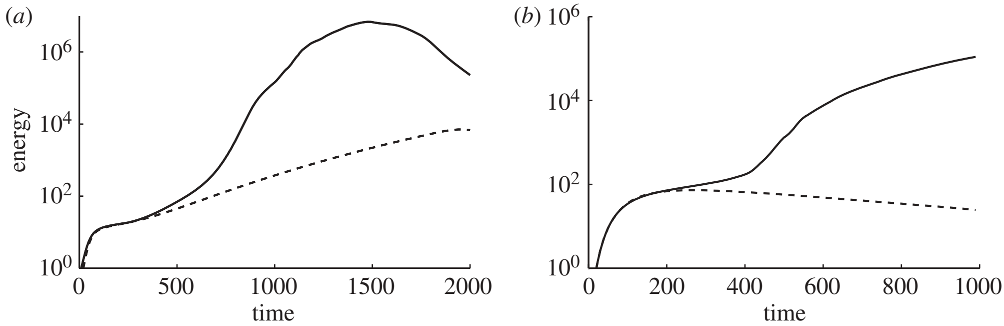

Figure 2. The time evolution of the disturbance kinetic energy corresponding to a nonlinear simulation (solid line) and linear simulation (dashed line). (*a*) TS wavepacket and (*b*) streak wavepacket.

instances in time[1] using the λ_2-criterion [4]. The small amplitude and nearly two-dimensional disturbance gradually evolves into a localized turbulent spot with a typical arrow-shaped structure.

A second type of disturbance is streamwise vortices with a dominant spanwise length scale and nearly uniform extension in the streamwise direction (figure 1*b*). To trigger turbulence, these streaks require significantly higher amplitudes (10% of the free-stream velocity) than TS wavepackets and can experience orders of magnitude of growth at relatively low Reynolds numbers (around 10^5), through the so-called lift-up mechanism. As shown in figure 1*b*,*d*,*f*, the disturbance characterized by streaky elongated structures eventually breaks down and evolves into a turbulent spot further downstream. In figure 2, the time evolution of the disturbance kinetic energy is shown with a black solid line for the TS wavepacket (figure 2*a*) and for the streak (figure 2*b*). The energy growth of the two disturbances is characterized by completely different growth rates and temporal scales: whereas the TS wavepacket grows at an exponential rate and breaks down at $t \approx 500$, the streaks grow at an algebraic rate with a much earlier breakdown at $t \approx 200$.

(*b*) *Transition control*

It is thus clear that, although the two disturbances meet the same fate, their spatial (shape and size) and temporal features are very different. As a consequence, flow-control studies have exploited the specific disturbance structure by introducing other disturbances that counteract either the TS waves or the streaks. For example, a second wave of appropriate amplitude and phase would cancel the TS travelling wave by interference or blowing and suction at the wall would cancel out the streaks. However, in many practical transition situations, we have to assume that we don't know the exact form of the disturbance and different disturbance types can be present in the flow at the same time.

[1]In this paper, time is normalized with the free-stream velocity U and the displacement thickness δ_0^*.

From a control viewpoint, the two transition scenarios have three salient features in common. If the upstream disturbances in the boundary layer are sufficiently small, the initial stage in the transition process is a *linear* amplification. In figure 2, the kinetic energy of a disturbance with an infinitesimal amplitude—where the nonlinear effects are neglected—is shown by the dashed line. We observe that the energy of the infinitesimal amplitude disturbance and the finite-amplitude disturbance initially grow with the same rate for both the TS wavepacket and the streak.

The second common feature is that significant amplification of disturbances—usually several orders of magnitude—takes place, but disturbances eventually propagate out of the flow domain and leave behind the steady boundary-layer flow. Moreover, disturbances propagate only in the downstream direction since any upstream travelling structure is quickly damped. This behaviour can be viewed as the transient growth of disturbance energy inflicted by the non-normality of the stable linear system.

The third feature of wall-bounded transitional flows that has vital implications for control design is the *time delay* (at the convective time scale) for the effects of an action on the flow to be measurable at a downstream location (e.g. [5]). As we shall see, systems with time delays are often challenging to control with very few degrees of freedom. In the present context, transition control focuses on a linear system governing the dynamics of small amplitude disturbances near the laminar solution, where the aim is to reduce the sensitivity of the system (i.e. the amplifying behaviour) with significant time delays as constraints.

2. Linear control systems

A large number of physical systems have the above features (linearity, sensitivity and time delays) in common, and there is a complete and rigorous theory that is able to provide us with optimal and robust controllers in order to manipulate the system behaviour. The indisputably largest challenge in using linear control theory for transition delay is to find a practical mathematical model of the perturbation dynamics, the sensors and the actuators. The linearized Navier–Stokes equations describe all aspects of the disturbance, but once discretized, they lead to a very large model, with 10^5–10^8 d.f. depending on the flow configuration. Such complex models do not lend themselves in a straightforward manner to control design; it is too expensive to apply standard control theoretical tools to models larger than 10^4. Even if we could design a controller from a Navier–Stokes model, it would have the same high dimension as the model, and, therefore, difficult to implement in experiments and too slow to run in real time.

In this paper, we review two approaches to obtain a feasible model of the fluid flow

— develop a set of low-dimensional subsystems from the Navier–Stokes equations, by exploiting some physical insight (e.g. spatial invariance of the flow) and
— develop one low-dimensional model that preserves only the important dynamical aspects for control design, either by systematically reducing the order of the Navier–Stokes equations, or by using system-identification techniques.

Before we discuss the above methods in more detail, we provide the setting for control design: the starting point is to formulate the linear flow, including sensors, actuators, disturbances and objective functions in state-space form,

$$\dot{\mathbf{q}}(t) = A\mathbf{q}(t) + B\mathbf{u}(t) \tag{2.1a}$$

and

$$\mathbf{y}(t) = C\mathbf{q}(t) + D\mathbf{u}(t). \tag{2.1b}$$

The state vector is denoted by $\mathbf{q} \in \mathbb{R}^n$, where n is the dimension of the state-space system and the constant matrix A governs the linear dynamics of the state. If the above system is derived from the Navier–Stokes equations, then $\mathbf{q}$ is the perturbation velocity, A is the discretized and linearized Navier–Stokes equations including boundary conditions and $n = 3n_x n_z n_y$, where n_x, n_y and n_z are the number of grid points in the x-, y- and z-directions, respectively. However, it is not always possible to attach a physical meaning to the state-space formulation (for instance, if system-identification techniques are used).

Any external influence on the flow contained in the forcing term $B\mathbf{u}(t)$ is decomposed into a spatial component B and a temporal signal $\mathbf{u} \in \mathbb{R}^m$, where m is the number of inputs. In the simplest control configuration, $m = 2$, representing one disturbance and one actuator, but often for three-dimensional flows, m is substantially larger, as more than one actuator and disturbance are active at the same time. Any information extracted from the flow is contained in the output signal term $\mathbf{y} \in \mathbb{R}^p$, where the constant matrix C determines where in the spatial domain flow measurements are extracted. Again, in the simplest control system, $p = 2$, in order to include one output equation for the sensor measurements used to *detect* the flow disturbances that we wish to control and one output equation to quantify the *performance* of the control system. The norm of the latter output defines a control objective function J,

$$J(T) = \|\mathbf{y}\|^2 = \int_0^T \mathbf{q}^* C^* C\mathbf{q} + \mathbf{u}^* D^* D\mathbf{u}\,\mathrm{d}t. \tag{2.2}$$

Finally, D represents a feed-through term that describes how the input can affect the output, for example to penalize the control effort in J.

3. Distributed control for spatially invariant systems

A large number of studies have exploited the spatial invariance (or the nearly spatial invariance) of certain flow configurations to derive state-space formulations that are applicable to control theoretical tools. Consider channel flow with two homogeneous directions (x, z) and one inhomogeneous direction (y). By expanding the perturbation into a set of Fourier functions in the x- and z-directions, it can be decoupled into a sequence of wavenumber pairs (k, l), where the two fundamental wavenumbers are defined as $\alpha_0 = 2\pi/L_x$ and $\beta_0 = 2\pi/L_z$. As observed by Joshi *et al.* [6], the decoupling of the perturbation into

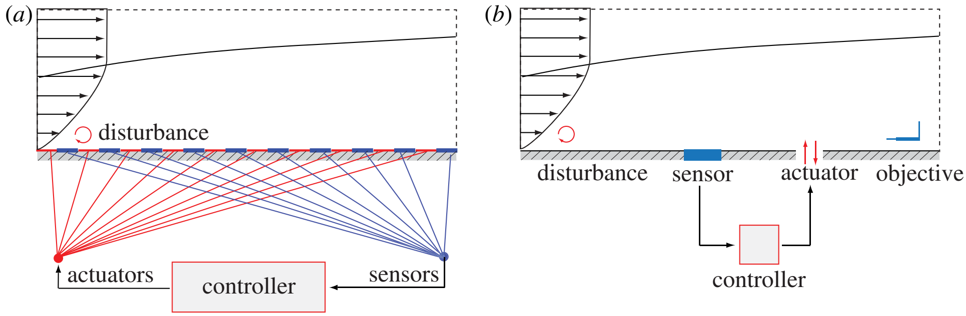

Figure 3. Schematic figures of control configurations with (*a*) distributed control and (*b*) localized control. In (*a*), the sensors and actuators are evenly distributed on the wall. The control can act in either Fourier space (centralized control) or in physical space (decentralized control). In (*b*), only a few sensors and actuators with compact spatial support are employed. (Online version in colour.)

wavenumber pairs is transferred to the system matrix A, which now has a block diagonal form,

$$A = \mathrm{diag}\{A_{1,1}, \ldots, A_{k,l}, \ldots, A_{K,L}\}. \tag{3.1}$$

Each of the block matrices $A_{k,l}$ represent the familiar Orr–Sommerfeld/Squire equations with the dimension $n = n_y$, i.e. the number of grid points in the wall-normal direction only. If one further assumes that inputs and outputs are evenly distributed in x and z, then the input (B) and output (C) vectors for each wavenumber pair are also decoupled from one another,

$$B = [B_{1,1}, \ldots, B_{k,l}, \ldots, B_{K,L}] \quad \text{and} \quad C = [C_{1,1}, \ldots, C_{k,l}, \ldots, C_{K,L}]^{\mathrm{T}}. \tag{3.2}$$

This means that instead of a three-dimensional state-space problem (2.1), one can formulate a set of one-dimensional problems,

$$\dot{\mathbf{q}}_{k,l}(t) = A_{k,l}\mathbf{q}_{k,l}(t) + B_{k,l}\mathbf{u}_{k,l}(t) \tag{3.3a}$$

and

$$\mathbf{y}_{k,l}(t) = C_{k,l}\mathbf{q}_{k,l}(t) + D_{k,l}\mathbf{u}_{k,l}(t), \tag{3.3b}$$

for $k = 1, \ldots, K$, $l = 1, \ldots, L$ and $n = n_y \leq 10^2$. Distributed control and sensing (for example, blowing/suction and shear-stress measurements at the wall), require thus KL actuators and sensors, i.e. one actuator and one sensor for each grid point at the wall (see sketch in figure 3*a*). So in this formulation, the number of inputs (m), outputs (p) and state (n) are of the same order.

Joshi *et al.* [6] were able to stabilize single wavenumber pairs of the linearly unstable Poiseulle flow using optimal linear feedback control (linear quadratic Gaussian; LQG) design together with boundary control (blowing/suction) and sensor measurement at the wall. In a similar way, Bewley & Liu [7] controlled the transient growth of individual stable wavenumber pairs using modern robust and optimal control theory. These two seminal investigations paved the way for future researchers as they took into account unknown and variable disturbances in imprecise flow conditions, mathematical modelling of boundary actuation, optimality and robustness (LQG/$\mathcal{H}_\infty$ methods), minimal realizations (controllability and observability) and so on.

(*a*) *Centralized approach*

The first real attempt to control subcritical transition, based on the approach discussed above, was by Cortelezzi *et al.* [8] in a two-dimensional periodic channel at $Re = 10^4$. The order of the full system (2.1) was $n \approx 10^4$, but could be decoupled to 32 subsystems (3.3) of order less than 10^2. The authors designed one controller for each wavenumber, such that, given shear-stress measurements at each point at the wall, the controller provided the blowing/suction signal at that point so that the shear stress was minimized and the control effort was penalized. Since the controllers are active in Fourier space, the physical wall measurements must first be converted via a fast Fourier transform (FFT) into Fourier space before they are fed to the controllers; to obtain the blowing/suction signal, the control signals have to be transformed back to physical space via an inverse FFT. Using this approach, Cortelezzi *et al.* [8] were able to reduce the wall-shear stress up to 90 per cent when the system was excited with optimal initial conditions, leading to the largest possible transient growth of shear stress. Lee *et al.* [9] extended the controller into the spanwise direction in an ad hoc manner and applied it to the turbulent channel flow at $Re_\tau = 100$. They were able to reduce the turbulent drag by 17 per cent.

(*b*) *Decentralized approach*

The major shortcoming with the so-called centralized approach adopted by Cortelezzi *et al.* [8] is that the computational cost of the FFT and inverse FFT increases rapidly with the number of wavenumbers. This issue was addressed in a set of consecutive papers from the Royal Institute of Technology and University of California, San Diego, flow-control groups (e.g. [10]). These authors adopted a decentralized approach, where instead of the signals, the controllers themselves were transformed back into physical space, after being designed in Fourier space. This approach results in so-called convolution kernels, which are computed only once and then used in physical space to provide control signals directly from measurements. The decentralized approach is justified by the theoretical predictions by Bamieh *et al.* [11]. These authors showed that for spatially invariant systems with distributed controls and measurements, controllers obtained by solving a set of smaller problems in Fourier space are spatially localized in physical space. Several successful projects were initiated to extend this approach to weakly spatially developing flows [12,13] and even to fully turbulent flows [14].

With regard to transition control of the flat-plate boundary layer, this series of work started with the application of full information control (i.e. assuming we can measure the entire flow field at all times) in Högberg & Henningson [15], it continued with detailed investigations of stochastic models for external sources of excitations in Hœpffner *et al.* [16], and it finally culminated in the partial information control in Chevalier *et al.* [12]. The use of stochastic disturbance models allowed computation of well-behaved estimation feedback kernels for three wall measurements: the two components of the skin friction and the wall pressure. The combination of the three measurements, albeit extracted on the wall, is able to estimate the full flow remarkably well, as demonstrated in figure 4. Chevalier *et al.* [12] showed that using this setup, in a boundary layer at transitional Reynolds numbers, the exponential growth of

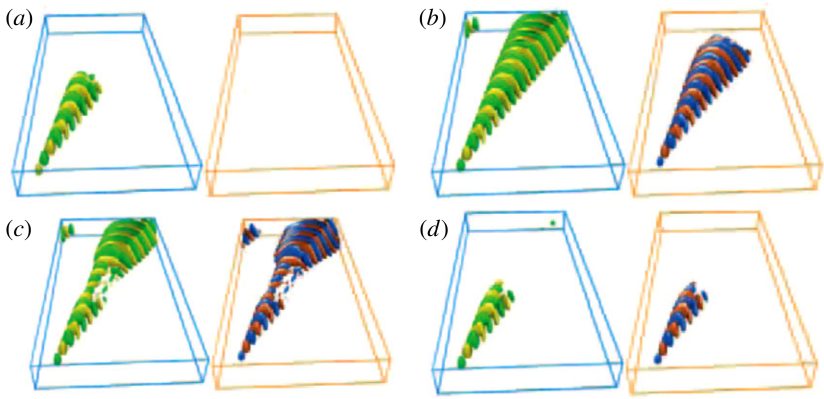

Figure 4. Optimal feedback control of small-amplitude oblique waves developing in the flat-plate boundary layer, visualized with iso-contour levels of the streamwise velocity component. In each frame, the left-hand boxes (blue boxes online) represent the true flow, whereas the right-hand boxes (brown boxes online) represent the estimated flow. In (*a*), a snapshot of the disturbance is shown with no control/estimation active. In (*b*), only the estimator is active, where, based only on wall measurements, the disturbance in the full domain can be fully reconstructed. In (*c*), the controller is active, resulting in a disruption of the travelling wave. Finally, in (*d*), the controller has been active for a sufficiently long time to suppress the disturbance. (Online version in colour.)

small-amplitude two-dimensional TS waves could be suppressed by two to three orders of magnitude, and the algebraic growth of streamwise streaks could be damped by a factor of two. In these studies—due to the compact support of the feedback kernels—a small spanwise strip of the flat plate could be used for sensing and actuation.

The true significance of damping small-amplitude perturbations for transition delay was shown in direct numerical simulations and large-eddy simulations by Monokrousos *et al.* [13] of the flat plate in the presence of free-stream turbulence ($Tu = 4.7\%$). As shown in figure 5, the decentralized feedback controller, which uses only small strips of the flat plate for sensing and control, is able to delay the entire transition process by damping the linear growth of perturbations, despite the presence of strong nonlinear effects.

Although numerical simulations (as shown in figures 4 and 5) have shown the efficiency of distributed feedback control, several shortcomings have rendered it difficult for experimental implementation

— it introduces a very high-dimensional controller or it requires online Fourier transforms,
— strictly speaking, it is only applicable to spatially invariant systems, and
— it is based on the assumption of an even distribution of sensors and actuators.

As we mentioned earlier, with regard to the first point, high-order controllers are inefficient in applications; today, we lack methods to reduce the order of very high-dimensional controllers in a systematic way, as the methods

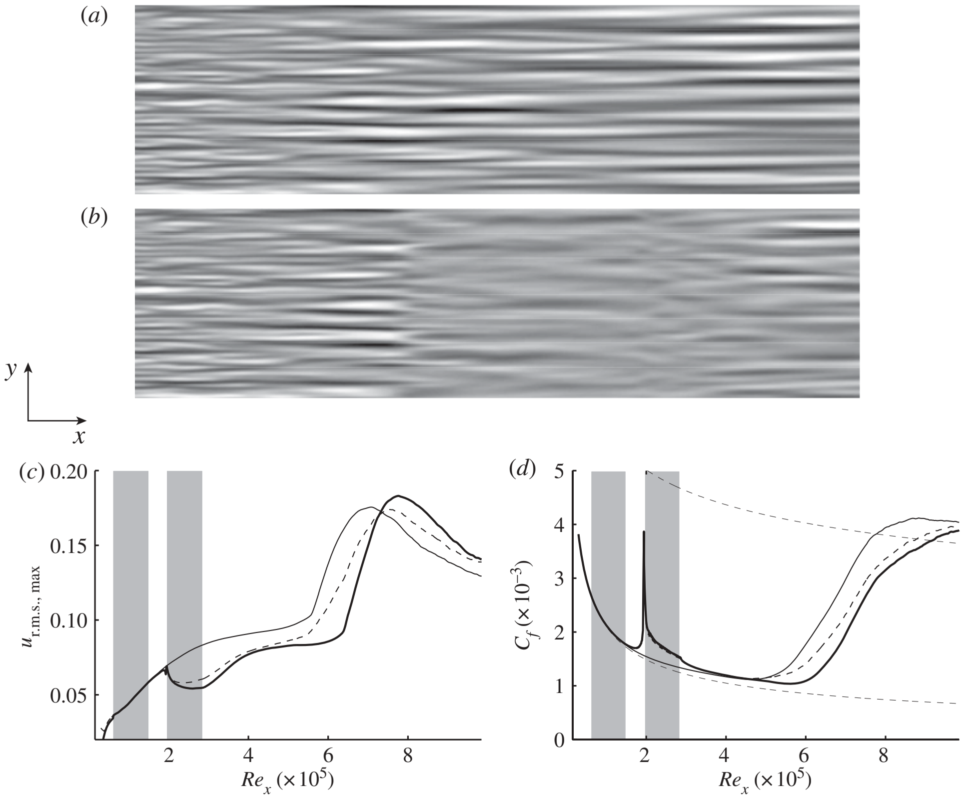

Figure 5. Optimal feedback control of transition induced by free-stream turbulence using a 'strip' of actuation (blowing/suction) and of sensing (shear stress) on the wall. (a,b) Instantaneous views of the streamwise velocity component in a parallel plane close to the wall, (a) without and (b) with feedback control are shown. Re_x ranges from 32 000 to 382 000. The reduction of the streak amplitude is clearly visible. A turbulent spot appears further downstream in the uncontrolled flow, while the flow is laminar when blowing/suction is applied. (c) The wall-normal maximum of the r.m.s. value of the streamwise velocity perturbation is shown for the uncontrolled case and for both full information control and compensation. (Thin line, no control; thick line, full information control; dashed line, estimation-based control.) (d) The corresponding skin-friction coefficient confirms the transition delay. (Thin line, no control; thick line, full information control; dashed line, estimation-based control.) Adapted from Monokrousos *et al.* [13].

developed in the control community are only applicable to controllers of moderate size. The second point is a severe restriction; even if the approach can be extended to weakly spatially developing flows, more complex flows, such as flows in ducts, corners, diffusers and on elliptic leading edges are out of reach. Finally, the assumption of distributed sensors and actuators restricts the approach to acting and sensing devices that can be manufactured in very large numbers such as microelectromechanical systems type of technology, whereas in many applications, this is not cost efficient, and only a few localized sensors and actuators suffice to manipulate the flow in a desired way.

4. Localized control of spatially developing systems

In this section, we present the 'next-generation' techniques for a linear systems approach to transition control that addresses the limitations of the methods in §3 in a direct and efficient way. The most important feature of the techniques outlined and reviewed herein is that they do not rely on physical insight into the specific flow configuration, and can, in principle, be applied to any geometry. Moreover, there are no assumptions about the shape and distribution of actuators and sensors.

Transitional wall-bounded flows are strongly convection dominated, which means that there is a very limited amount of information propagating upstream. A natural setup of localized actuators and sensors for such flows is sketched in figure 3*b*. The disturbance is measured by a set of detection sensors placed upstream of a set of actuators. The sensor signals are fed through a low-order controller before driving the actuators. Finally, a set of 'error' sensors downstream of the actuators is introduced. The output of the error sensors can be used to monitor the performance of the active control source and the objective of the control system is the minimization of this error signal.[2] It is important to place actuators and sensors at appropriate locations to be able to capture important dynamics and to manipulate the flow with small amounts of energy. For convection-dominated flows, there are no systematic methods available to choose optimal actuator and sensor locations and a trial-and-error procedure is usually employed.

The present approach is based on the recognition that, based on whatever filtered information delivered from the measured *output* signals to the controller, suitable *input* signals are determined to achieve the desired flow behaviour. Thus, of importance for control design is to extract the components necessary to describe the relation between input and output time signals from the Navier–Stokes equations. This input–output dynamics is often much simpler than the full spatio-temporal perturbation dynamics. There are two approaches to find a model of the input–output dynamics instead of the full perturbation dynamics: (i) the use of model-reduction techniques to systematically reduce the complexity of the Navier–Stokes system and extract the input–output dynamics and (ii) the use of system-identification techniques to develop a mathematical model directly from measurement, with no regard to the Navier–Stokes equations.

(*a*) *Model reduction via Galerkin projection*

The model-reduction technique discussed here falls into the category of projection methods, where one projects the Navier–Stokes system onto an appropriate low-dimensional subspace spanned by a set of flow fields, called modes. For instance, expanding the state vector $\mathbf{q}(t)$ in a set of basis functions $\boldsymbol{\phi}_i$, we have

$$\mathbf{q}(t) = \sum_{i=1}^{r} a_i(t)\boldsymbol{\phi}_i, \tag{4.1}$$

[2] The term feedback control is interpreted in different ways by different segments of the control community. From an electrical engineering viewpoint, the set-up sketched in figure 3*b* can be interpreted as feedforward, since the action of the actuators affects only the signal measured at the downstream sensors and not the upstream sensors.

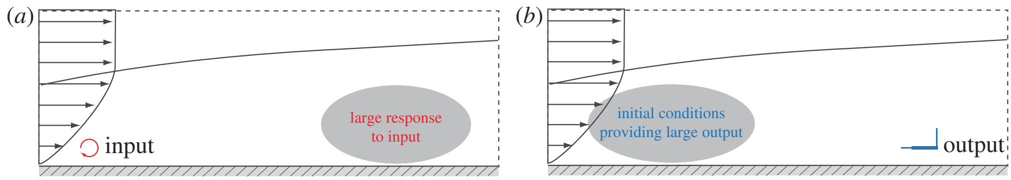

Figure 6. Sketch of (*a*) controllability and (*b*) observability for the flat-plate boundary layer. The response to an input is large downstream (because of strong convection), which results in a large controllability of flow structures in the downstream part of the domain. Similarly, the flow structures that will, after a transient time, result in a large sensor output are located far upstream, resulting in strong observability in that region. (Online version in colour.)

where $r \ll n$. If the basis is orthonormal, the expansion coefficients $a_i(t)$ are given by $a_i(t) = \langle \mathbf{q}(t), \boldsymbol{\phi}_i \rangle$, but if it is not orthonormal, they are given by $a_i(t) = \langle \mathbf{q}(t), \boldsymbol{\psi}_i \rangle$, where $\boldsymbol{\psi}_i$ is the adjoint mode, satisfying the bi-orthogonality condition $\langle \boldsymbol{\phi}_j, \boldsymbol{\psi}_i \rangle = \delta_{ij}$. By inserting the above expansion into equation (2.1) and using the bi-orthogonality condition, we get

$$\dot{a}(t) = A_r a(t) + B_r \mathbf{u}(t) \tag{4.2a}$$

and

$$\mathbf{y}_r(t) = C_r a(t) + D\mathbf{u}(t), \tag{4.2b}$$

where $a(t) = [a_1(t), \ldots, a_r(t)] \in \mathbb{R}^r$, and $A_r \in \mathbb{R}^{r\times r}, B_r \in \mathbb{R}^r, C_r \in \mathbb{R}^r$ are small matrices that define the reduced-order model. In projection methods, the dynamics captured by the reduced-order model depends on the choice of expansion basis $\boldsymbol{\phi}_i$ and the direction of projection, determined by the adjoint basis $\boldsymbol{\psi}_j$. The expansion basis can be eigenvectors of the linearized Navier–Stokes system [17] or different varieties of proper orthogonal decomposition (POD) modes [18].

One of the most common model-reduction techniques in the linear control community is balanced truncation [19]. The method is based on the important notions of controllability and observability; concepts that are significant when inputs and outputs are introduced. In particular, for a given input, say blowing/suction through an orifice, controllability addresses the question which flow fields are most easily triggered by the input. Similarly, for a given output, say shear-stress wall measurements, observability addresses the question which flow fields contribute the most to the output measurements. In figure 6, the regions in the flow domain where controllability and observability are significant is sketched for wall-bounded flows. These so-called controllable and observable states can be identified from the spatial correlation matrices (also called Gramians) of the linear system (2.1) and an associated dual (or adjoint) system. The projection basis $\boldsymbol{\phi}_j$ and its associated adjoint basis $\boldsymbol{\psi}_j$ are then computed by diagonalizing the product of the two Gramians.

Controllability and observability were considered already by early investigators in this field [6–9], but not for the specific aim of reducing the complexity of the Navier–Stokes equations. At that time, a numerical algorithm to apply this technique directly on Navier–Stokes equations was not available. Inspired by the so-called snapshot technique Sirovich [20] used to compute POD modes, Lall *et al.* [21] and Willcox & Peraire [22] made significant progress in developing

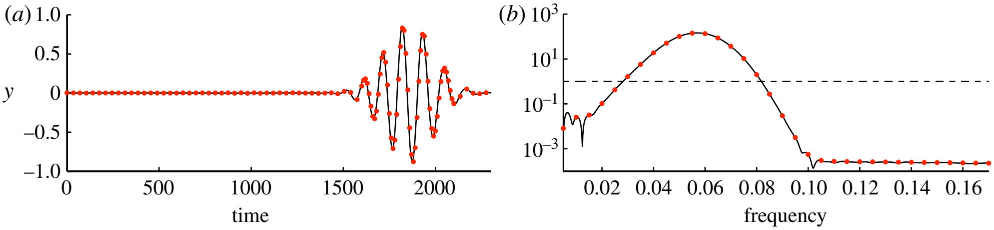

Figure 7. (*a*) Impulse and (*b*) frequency response of the flat-plate boundary layer when the system is forced far upstream and measured far downstream. The solid lines show responses from direct numerical simulation computations ($n \approx 10^5$). The filled circles (red symbols online) show the responses from the reduced-order model ($r = 60$). Adapted from Bagheri *et al.* [27]. (Online version in colour.)

balanced truncation for very high-dimensional systems and nonlinear systems. Finally, Rowley [23] was able to reduce the computation of the balanced truncation method from a large eigenvalue problem to a relatively small singular value decomposition problem. This so-called *snapshot-based balanced truncation method* can be applied to reduce the complexity of very high-dimensional systems (order $n \approx 10^4$–10^8), if the number of inputs and outputs are considerably smaller, i.e. $m, p < 10^2$. So far, this method has been validated against exact balanced truncation techniques and compared with other ad hoc model-reduction techniques based on POD modes on the channel flow [24], the Ginzburg–Landau equation [25] and the problem of incompressible cavity flow [26].

Using a simple two-dimensional setup (two sensors, one actuator and one disturbance as in figure 3*b*), Bagheri *et al.* [27], showed that a significant order reduction can be combined with control theoretical tools to attenuate disturbances in spatially developing flows. In figure 7, the sensor signal of the Navier–Stokes system (solid line) is compared with the signals of the reduced-order model (filled circles) when the two systems are forced with an impulse (figure 7*a*) and harmonic signals (figure 7*b*). From the impulse response, we can observe a time delay of 1500 time units before the sensors give a significant output. From the frequency response, we can see that a wide range of frequencies ($\omega \in [0.03, 0.08]$) are amplified, whereas low and high frequencies are damped. To capture both the time-delay effects and the broad-band spectrum with a high accuracy, at least 60 d.f. is necessary. The reduced order was used to design a small optimal feedback controller, which could damp the energy of the two-dimensional TS wavepackets forced upstream by orders of magnitudes. A similar analysis was performed by Bagheri *et al.* [28], where instead of body forces, blowing/suction actuators and wall-shear stress were employed. However, the fact that the inputs and outputs were modelled as a body force does not mean that they were unrealistic. It is the effect of an actuator that is important to model, and not the actuator itself. Therefore, the action that the body force has on the flow could possibly be reproduced, for example using plasma actuators.

The input–output approach can be extended to a fully three-dimensional configuration [29,30]. In the homogeneous spanwise direction of the flat plate, an array of localized sensors, followed by an array of actuators further downstream are distributed near the rigid wall. The objective is to minimize the perturbation

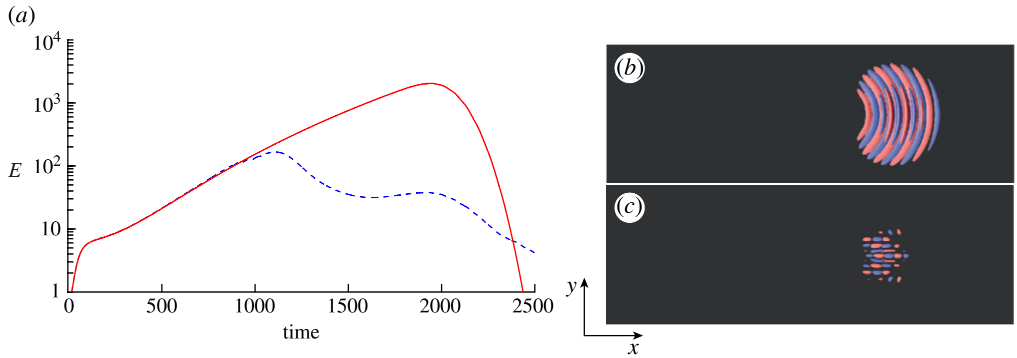

Figure 8. (a) Kinetic energy of a three-dimensional disturbance in the flat-plate boundary layer without (solid line) and with (dashed line) feedback control. In the uncontrolled flow, an exponential growth of three orders of magnitude is observed. The disturbance energy of the closed-loop system obtained using a low-order ($r = 60$) controller has about one order of magnitude smaller peak energy. Instantaneous snapshots of the disturbance field (b) without and (c) with feedback control, demonstrate the effect of the controller: the two-dimensional structure of the disturbance in (b) has been replaced by a smaller scale three-dimensional disturbance in the closed-loop system (c). (Online version in colour.)

energy in a spatial domain spanned by a number of prudently chosen output equations; for example, the leading 10 POD modes generated from the impulse response of the disturbances or a number of localized Fourier modes. Reduced-order ($r \approx 60$) optimal controllers developed from balanced truncation models, are able to reduce the growth of complicated three-dimensional disturbances by orders of magnitudes as demonstrated in figure 8. In this particular configuration, nine sensors and nine actuators were used to control the exponential growth of the three-dimensional TS wavepacket discussed in §1. An efficient control performance is also observed for the control of streaks (energy growth reduced by a factor of two). However, since streaks reach their maximum energy faster (figure 2) and have smaller spanwise scales compared with TS wavepackets, the actuators and sensors are placed closer to each other in the spanwise direction and are moved further upstream in the streamwise direction. It is interesting to note, however, that the same physical shape of sensors and actuators can be used to control both TS and streak wavepackets, indicating that it is not necessary to design disturbance-specific devices to develop efficient controllers.

(b) *System-identification methods*

System identification is a well-established mathematical field, with the aim of modelling systems from experimental measurements. In its simplest form, it is performed by exciting a system (with an impulse, a step or a harmonic signal) and observing its inputs and outputs over a time interval, followed by finding a model that fits the input–output relation. The latter step is usually performed by a statistically based method to estimate unknown parameters of the system.

A simple example of model parametrization is the 'Autogression with exogenous input model'. Given a sequence of input and output signals at discrete times,

$$[\mathbf{u}(t_1), \mathbf{u}(t_2), \ldots, \mathbf{u}(t_k)] \quad \text{and} \quad [\mathbf{y}(t_1), \mathbf{y}(t_2), \ldots, \mathbf{y}(t_k)], \tag{4.3}$$

the output at the current time t_{k+1} can be written as a linear combination of the previous input and output samples,

$$\mathbf{y}(t_{k+1}) = -\sum_{j=1}^{r} E_j \mathbf{y}(t_j) + \sum_{j=1}^{r} F_j \mathbf{u}(t_j). \tag{4.4}$$

The unknown parameters $E_i \in \mathbb{R}^{p\times p}$ and $F_i \in \mathbb{R}^{p\times m}$ are chosen such that the difference between the output of the experiments and the model output given the same input sequence is minimized in a least-square sense.

Since these models are developed purely from measurement signals for various input signals, they capture the input–output dynamics, similarly to balanced truncation. In fact, it was recently realized [31] that a common system-identification algorithm [32] produces exactly the same reduced-order models as snapshot-based balanced truncation. Neither simulations of the adjoint system nor a Galerkin projection onto expansion basis are necessary to obtain low-order state-space models. This equivalence is true only if the underlying system is linear (which is certainly not the case in experiments). If the true flow behaviour is nonlinear, the identified linear model may not converge to it, since a nonlinear model cannot be represented by one single linear model, regardless of the length of sampled input–output signals used. So, it is not always certain that system-identification models can provide effective linear controllers since unmodelled nonlinear dynamics may severely limit the performance.

A number of successful experimental investigations (e.g. [33,34]) of transition delay have been conducted using system-identification techniques. For instance, Rathnasingham & Breuer [35] used a set-up similar to the sketch in figure 3*b*: an array of three shear-stress sensors were placed upstream of three synthetic jets actuators followed by three error sensors far downstream. The linear controller was based on stochastically estimated transfer functions between the inputs and outputs, and the control objective was to minimize the difference between the predicted signal of the estimated linear model and the true signal from the experiments. They were able to reduce the streamwise velocity fluctuations and the mean wall shear stress in a turbulent ($Re_x = 8\times 10^5$) boundary layer by 30 per cent and 7 per cent, respectively. A similar localized set-up of sensors and actuators was employed in the wind-tunnel experiment by Lundell [36]. He investigated the effects of simple feedback control (when the measured shear stress was below a threshold, steady suction was applied after some time delay) on the behaviour of streaks excited by external free-stream turbulence.

There are a number of aspects of system-identification experiments that can be further improved using numerical simulations: (i) in Rathnasingham & Breuer [35] and Sturzebecher & Nitsche [34], the objective is to minimize the signals of few surface hot-wire sensors located far downstream in the boundary layer. In contrast to experiments, in model-based control, we are able formulate a control objective that encompasses much larger domains also further away from the wall, which enhances the control efficiency. (ii) The use of model-based estimation, such as the Kalman filter can significantly improve the estimation accuracy of the flow state. (iii) Numerical investigations can be useful for experiments by providing guidelines for the shape and spatial distribution of actuators and sensors. Therefore, one can set up experiments after first evaluating a large number of numerical simulations, in order to understand how to design and place actuators and sensors.

Similar to distributed control discussed in §3, the localized/input–output framework has its own set of drawbacks

- — the placement of the actuators and sensors at the wall is related to the spatial and temporal scales of the disturbances,
- — different choices of sensors used to define the objective function can yield different control results, and
- — the computational cost of model reduction and system-identification algorithms, as well as the experimental feasibility (i.e. wiring), increase rapidly with the number of inputs and outputs.

In contrast to distributed control, in localized control, the location of actuators and sensors in the streamwise direction and their spacing in the spanwise direction is different for the control of streaks and TS waves. In a similar way, the second point also makes the design disturbance specific. In experiments, output signals can only be extracted from sensor measurements, whereas in numerical simulation, a spatial domain spanned by an expansion basis (such as POD modes) can be used to define the output signals. In either case, the control performance depends on the choice of the output signals and some ‘engineering judgement’. The final point may become a severe restriction due to the second point, since defining an objective function that captures a significant amount of physical information might require a large number of sensors.

5. Conclusions

This paper summarizes the research efforts to combine linear control theory, hydrodynamic stability theory and numerical simulations to delay the transition to turbulence in wall-bounded shear flows. The emergence of this particular field in flow control is tightly coupled to the recent developments in direct numerical simulation techniques, novel ‘matrix-free’ algorithms as well as increasing computational resources. The control efficiency for attenuating small-amplitude disturbances is equally good for localized control, based on reduced-order models, as for distributed control based on convolution kernels. In the former approach, only a few small localized sensors and actuators are employed and considerable flow manipulation can be achieved by exploiting the large sensitivity typical of wall-bounded flows. In the latter approach, the nearly spatial invariance of the flow is instead exploited to evenly distribute sensors and actuators.

Although, linear control methods are particularly well suited for transition control, they have been successfully applied to related flow-control fields, where linear mechanisms are an essential part of the underlying physics. For example, the linear growth and breakdown of streaks discussed here in the context of transition are also observed in the regeneration cycle that has been proposed to sustain turbulence. Nevertheless, the wide range of scales in both space and time in turbulent flows renders it a significantly more difficult and 'nonlinear' control problem. A particular challenging task is to obtain an accurate estimate of a turbulent flow using linear estimation techniques by incorporating realistic and physical disturbance statistics both in space and time. Linear mechanisms also play a fundamental role in separated flows or for flows that exhibit supercritical transition, such as the Hopf bifurcation in a cylinder wake. For such flows, linear control can provide efficient means to stabilize the unsteady self-sustained oscillations well above critical Reynolds numbers (e.g. [26]).

Since Joshi *et al.* [6] introduced linear control theory to the fluid-mechanics community, the number of research projects in this vein has increased at an exponential rate. These studies—although purely theoretical or performed on simple models—has brought us to a stage where the numerical development of reliable controllers is possible to use in the laboratory experiments and eventually in more complicated technological configurations. An equally important contribution to this is the large number of experimental flow-control studies devoted to the development and fabrication of flow-measurement and actuation devices, as well as physical implementation of active controller algorithms.

References

1 Gal-El-Hak, M. 1996 Modern developments in flow control. *Appl. Mech. Rev.* **49**, 365–379. (doi:10.1115/1.3101931)

2 Bewley, T. R. 2001 Flow control: new challenges for a new renaissance. *Prog. Aerospace. Sci.* **37**, 21–58. (doi:10.1016/S0376-0421(00)00016-6)

3 Kim, J. & Bewley, T. R. 2007 A linear systems approach to flow control. *Annu. Rev. Fluid Mech.* **39**, 383–417. (doi:10.1146/annurev.fluid.39.050905.110153)

4 Jeong, J. & Hussain, F. 1995 On the identification of a vortex. *J. Fluid Mech.* **285**, 69–94. (doi:10.1017/S0022112095000462)

5 Naguib, A. M., Morrison J. F. & Zaki, T. A. 2010 On the relationship between the wall-shear-stress and transient-growth disturbances in a laminar boundary layer. *Phys. Fluids* **22**, 054103. (doi:10.1063/1.3415220)

6 Joshi, S. S., Speyer, J. L. & Kim, J. 1997 A systems theory approach to the feedback stabilization of infinitesimal and finite-amplitude disturbances in plane poiseuille flow. *J. Fluid Mech.* **332**, 157–184.

7 Bewley, T. R. & Liu, S. 1998 Optimal and robust control and estimation of linear paths to transition. *J. Fluid Mech.* **365**, 305–349. (doi:10.1017/S0022112098001281)

8 Cortelezzi, L., Speyer, J. L., Lee, K. H. & Kim, J. 1998 Robust reduced-order control of turbulent channel flows via distributed sensors and actuators. In *IEEE 37th Conf. on Decision and Control, Tampa, FL, December 1998*, pp. 1906–1911.

9 Lee, K. H., Cortelezzi, L., Kim, J. & Speyer, J. 2001 Application of reduced-order controller to turbulent flow for drag reduction. *Phys. Fluids* **13**, 1321–1330. (doi:10.1063/1.1359420)

10 Högberg, M., Bewley, T. R. & Henningson, D. S. 2003 Linear feedback control and estimation of transition in plane channel flow. *J. Fluid Mech.* **481**, 149–175. (doi:10.1017/S0022112003003823)

11 Bamieh, B., Paganini, F. & Dahleh, M. 2002 Distributed control of spatially invariant systems. *IEEE Trans. Automat. Control* **47**, 1091–1107. (doi:10.1109/TAC.2002.800646)

12 Chevalier, M., Hœpffner, J., Åkervik, E. & Henningson, D. S. 2007 Linear feedback control and estimation applied to instabilities in spatially developing boundary layers. *J. Fluid Mech.* **588**, 163–187. (doi:10.1017/S0022112007007392)

13 Monokrousos, A., Brandt, L., Schlatter, P. & Henningson, D. S. 2008 DNS and LES of estimation and control of transition in boundary layers subject to free-stream turbulence. *Int. J. Heat Fluid Flow* **29**, 841–855. (doi:10.1016/j.ijheatfluidflow.2008.03.009)

14 Högberg, M., Bewley, T. R. & Henningson, D. S. 2003 Relaminarization of $Re_tau = 100$ turbulence using gain scheduling and linear state-feedback control flow. *Phys. Fluids* **15**, 3572–3575. (doi:10.1063/1.1608939)
15 Högberg, M. & Henningson, D. S. 2002 Linear optimal control applied to instabilities in spatially developing boundary layers. *J. Fluid Mech.* **470**, 151–179. (doi:10.1017/S0022112002001702)
16 Hœpffner, J., Chevalier, M., Bewley, T. R. & Henningson, D. S. 2005 State estimation in wall-bounded flow systems. I. laminar flows. *J. Fluid Mech.* **534**, 263–294. (doi:10.1017/S0022112005004210)
17 Åkervik, E., Hœpffner, J., Ehrenstein, U. & Henningson, D. S. 2007 Optimal growth, model reduction and control in a separated boundary-layer flow using global eigenmodes. *J. Fluid. Mech.* **579**, 305–314. (doi:10.1017/S0022112007005496)
18 Noack, B., Afanasiev, K., Morzynski, M., Tadmor, G. & Thiele, F. 2003 A hierarchy of low-dimensional models for the transient and post-transient cylinder wake. *J. Fluid Mech.* **497**, 335–363. (doi:10.1017/S0022112003006694)
19 Moore, B. 1981 Principal component analysis in linear systems: controllability, observability, and model reduction. *IEEE Trans. Automat. Control* **26**, 17–32. (doi:10.1109/TAC.1981.1102568)
20 Sirovich, L. 1987 Turbulence and the dynamics of coherent structures I—III. *Quart Appl. Math.* **45**, 561–590.
21 Lall, S., Marsden, J. E. & Glavaski, S. 2002 A subspace approach to balanced truncation for model reduction of nonlinear control systems. *Int. J. Robust Nonlinear Control* **12**, 519–535. (doi:10.1002/rnc.657)
22 Willcox, K. & Peraire, J. 2002 Balanced model reduction via the proper orthogonal decomposition. *AIAA J.* **40**, 2323–2330. (doi:10.2514/2.1570)
23 Rowley, C. W. 2005 Model reduction for fluids using balanced proper orthogonal decomposition. *Int. J. Bifur. Chaos* **15**, 997–1013. (doi:10.1142/S0218127405012429)
24 Ilak, M. & Rowley, C. W. 2008 Modeling of transitional channel flow using balanced proper orthogonal decomposition. *Phys. Fluids* **20**, 034103. (doi:10.1063/1.2840197)
25 Bagheri, S., Hœpffner, J., Schmid, P. J. & Henningson, D. S. 2009 Input–output analysis and control design applied to a linear model of spatially developing flows. *Appl. Mech. Rev.* **62**, 020803. (doi:10.1115/1.3077635)
26 Barbagallo, A., Sipp, D. & Schmid, P. J. 2009 Closed-loop control of an open cavity flow using reduced-order models. *J. Fluid Mech.* **641**, 1–50. (doi:10.1017/S0022112009991418)
27 Bagheri, S., Brandt, L. & Henningson, D. S. 2009 Input–output analysis, model reduction and control design of the flat-plate boundary layer. *J. Fluid Mech.* **620**, 263–298. (doi:10.1017/S0022112008004394)
28 Bagheri, S., Åkervik, E., Brandt, L. & Henningson, D. S. 2009 Matrix-free methods for the stability and control of boundary layers. *AIAA J.* **47**, 1057–1068. (doi:10.2514/1.41365)
29 Semeraro, O., Bagheri, S., Brandt, L. & Henningson, S. 2009 Linear control of 3D disturbances on a flat plate. In *7th IUTAM Symp. Laminar–Turbulent Transition*, vol. 18, pp. 373–378.
30 Semeraro, O., Bagheri, S., Brandt, L. & Henningson, D. S. Submitted. Feedback control of three-dimensional optimal disturbances using reduced-order models. *J. Fluid Mech.*
31 Ma, Z., Ahuja, S. & Rowley, C. W. In press. Reduced-order models for control of fluids using the eigensystem realization algorithm. *Theoret. Comput. Fluid Dyn.* (doi:10.1007/s00162-010-0184-8)
32 Juang, J. & Pappa, R. S. 1985 An eigensystem realization algorithm for modal parameter identification and model reduction. *J. Guidance Con. Dyn.* **3**, 620–627. (doi:10.2514/3.20031)
33 Jacobson, S. A. & Reynolds, W. C. 1998 Active control of streamwise vortices and streaks in boundary layers. *J. Fluid Mech.* **360**, 179–211. (doi:10.1017/S0022112097008562)
34 Sturzebecher, D. & Nitsche, W. 2003 Active cancellation of Tollmien–Schlichting waves instabilities on a wing using multi-channel sensor actuator systems. *Int. J. Heat Fluid Flow* **24**, 572–583. (doi:10.1016/S0142-727X(03)00051-1)
35 Rathnasingham, R. & Breuer, K. S. 2003 Active control of turbulent boundary layers. *J. Fluid Mech.* **495**, 209–233. (doi:10.1017/S0022112003006177)
36 Lundell, F. 2007 Reactive control of transition induced by free-stream turbulence: an experimental demonstration. *J. Fluid Mech.* **585**, 41–71. (doi:10.1017/S0022112007006490)